



An integrated crustal velocity field for the central Andes

Eric Kendrick and Michael Bevis

School of Ocean and Earth Science and Technology, University of Hawaii, Honolulu, Hawaii 96822, USA
(kendrick@soest.hawaii.edu; bevis@soest.hawaii.edu)

Robert Smalley Jr.

Center for Earthquake Research, University of Memphis, 3890 Central Avenue, Suite 1, Memphis, Tennessee 38152, USA (smalley@ceri.memphis.edu)

Benjamin Brooks

School of Ocean and Earth Science and Technology, University of Hawaii, Honolulu, Hawaii 96822, USA
(bbrooks@soest.hawaii.edu)

[1] **Abstract:** We present an integrated velocity field for the central Andes, derived from GPS observations collected between January 1993 and March 2001 that eliminates the velocity bias between the South America-Nazca Plate Project (SNAPP) and central Andes GPS Project (CAP) velocity fields published by *Norabuena et al.* [1998] and *Bevis et al.* [1999]. The reference frame is realized by minimizing the motion of eight continuous GPS stations and one rover GPS station located in the stable core of the South American plate. The RMS horizontal motion of these stations is just 1.1 mm/yr. The amplitude of these residual motions is roughly compatible with expected levels of measurement error. In our new solution, five of the six SNAPP stations located just outside the orogenic belt are effectively stationary, and the velocities for adjacent CAP and SNAPP stations now agree at a level consistent with their formal uncertainties.

Keywords: GPS; geodetic; interseismic; velocity; Central Andes.

Index terms: Continental contractional orogenic belts; Crustal movements—intraplate; South America; Space geodetic surveys.

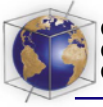
Received 13 June 2001; **Revised** 5 September 2001; **Accepted** 28 September 2001; **Published** 1 November 2001.

Kendrick, E., M. G. Bevis, R. Smalley, and B. A. Brooks, An integrated crustal velocity field for the central Andes, *Geochem. Geophys. Geosyst.*, 2, 10.1029/2001GC000191, 2001.

1. Introduction

[2] The Andes constitute the type example of a continental subduction zone. This highly seismogenic plate boundary is of great interest to seismologists observing the earthquake deformation cycle as well as to geologists and geo-

physicists studying the growth of mountain belts. As a result there are several groups engaged in GPS geodesy within the northern, central, and southern Andes. It is now widely recognized that a large fraction of the crustal velocity field in this region manifests elastic compression of the upper plate in response to

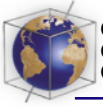


locking of the main plate boundary [Klotz *et al.*, 1999; Norabuena *et al.*, 1998; Bevis *et al.*, 1999]. However, back arc convergence also contributes to the Andean crustal velocity field [Norabuena *et al.*, 1998; Bevis *et al.*, 1999]. One of the main technical challenges for crustal motion geodesists working here, as in other convergent margins, is separating elastic end-loading signals produced by locking of the main plate boundary from other (possibly anelastic) components of the interseismic velocity field. The abrupt change in the trend of the Andes near 18°S, known as the Arica Deflection or the Bolivian Orocline, offers a special opportunity in this regard. The pronounced change in the orientation of the plate boundary, and in the obliquity of plate convergence [McCaffrey, 1994], will provide the elastic deformation field driven by plate boundary locking with an unusual signature that should help researchers to isolate this signal and thereby better isolate the motions and deformations associated with back arc convergence and perhaps oroclinal bending [Jordan *et al.*, 1983; Isacks, 1988; Gephart, 1994; Kley, 1999; Lamb, 2000].

[3] The central Andes GPS Project (CAP) [Kendrick *et al.*, 1999; Bevis *et al.*, 1999] and the South America-Nazca Plate Project (SNAPP) [Norabuena *et al.*, 1998] have been working in the central Andes since 1993 and 1994, respectively, and both groups have published preliminary velocity fields for parts of the central Andes. Unfortunately, an intercomparison of these solutions indicated a bias or offset between the two sets of velocity estimates. Bevis *et al.* [1999] suggested that this was due to a reference frame problem. In crustal motion geodesy the problem of realizing a fixed-plate reference frame and the problem of expressing velocities within that frame are highly coupled. When one tries to realize a fixed-plate frame using only a few GPS stations and/or a narrow time window, it

is difficult to suppress statistical fluctuations (measurement noise) that can generate complementary errors in the realization of the frame and in the expression of velocities relative to that frame. Norabuena *et al.* [1998] had only a 2 year time span of observations available to them for the SNAPP network, and they used only a few continuous GPS (CGPS) stations to realize a craton-fixed frame (one of which, International GPS Service (IGS) station KOUR, had data quality problems in the 1990s). Bevis *et al.* [1999] had a longer time series and more cratonic stations available to them than did Norabuena *et al.* [1998] for the purposes of realizing a craton-fixed frame.

[4] Both SNAPP and CAP will complete another occupation of their networks by the end of 2001. At that point there should be little difficulty in realizing essentially equivalent craton-fixed frames. However, we have made an effort to resolve the reference frame problem using data already in hand, both to produce an interim velocity field that can be used by us and by others engaged in modeling regional deformation and to throw more light onto the nature of the reference frame problem. While Norabuena *et al.* [1998] used GIPSY software and a point-positioning strategy, the CAP team uses GAMIT software and a network approach to position and velocity estimation. The network approach is probably the safer of the two approaches because it is redundant, and, when velocity estimation is implemented on a regional level (as described below), it eliminates spatially common-mode errors deriving from the global scale. Accordingly, we have reprocessed the SNAPP and CAP data sets jointly using GAMIT/GLOBK at the Pacific GPS Facility (PGF) of the University of Hawaii. We have more data available with which to realize a craton-fixed frame than did either Norabuena *et al.* [1998] or Bevis *et al.* [1999], and this should also assist us in elim-



inating the offset between crustal velocity fields previously reported for the CAP and SNAPP networks.

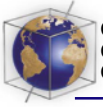
2. Realization of a South American Craton-Fixed Frame

[5] Our general processing strategy was described previously by *Kendrick et al.* [1999] and *Bevis et al.* [1999]. We estimate velocities by stacking daily network solutions (polyhedra) obtained using GAMIT [*King and Bock, 2000*] and GLOBK [*Herring, 2000*] software. In this section we explain our approach to velocity estimation in more detail and in terms that should be easy for the nongeodesist to follow.

[6] The basic GPS analysis is performed one day at a time using the distributed processing scheme [*Feigl et al., 1993; Oral, 1994; Zhang, 1996; Bock, 1998*] adopted by most GAMIT/GLOBK users. In effect, an analysis of the global GPS network of the IGS is combined with a separate analysis of our regional network, so as to achieve a solution which is essentially equivalent to that which would have been obtained if the two data sets had been merged and analyzed in one huge batch. The main advantages of the distributed approach are (1) that the total computational cost is greatly reduced and (2) that the regional analyst need not perform the global analysis but can concentrate instead on processing the regional data with GAMIT and combining the regional and global solutions using GLOBK. The resulting solution includes an estimate of the geometrical figure or polyhedron consisting of all global and regional GPS stations included in the daily analysis. Because the analysis (in its final stages) places only very weak constraints on the coordinates of these stations, the resulting “free network” solution is not strongly tied to any particular reference frame, and so while it

strongly constrains the size and shape of the polyhedron, it does not strongly constrain the position or orientation of this geometrical object [*Heflin et al., 1992; Blewitt, 1998*]. Free network solutions are also called “fiducial free,” “loose,” or “inner coordinate” solutions. Free network solutions describe the inner geometry of the polyhedron and do not address precisely how the polyhedron is embedded in an external reference frame thereby establishing its outer coordinates. The advantage of free network solutions is that they are very little influenced by any a priori information about the coordinates (and relative positions) of the various GPS stations. Even minor errors in prior coordinates used to impose a reference frame on a polyhedron are capable of inducing subtle distortions in the estimated shape of the polyhedron.

[7] A free network solution can be transformed into a description associated with a specific reference frame by applying a transformation consisting of three orthogonal translations and three orthogonal rotations. This six-parameter similarity transformation is known in geodesy as a Helmert transformation. (It is also possible to employ a seventh parameter to permit small changes in scale. This can be very useful when combining measurements made using different physical principles, e.g., optical versus radio techniques, to account for small inconsistencies in the various fundamental physical constants used in the different analyses or data reductions. However, it rarely makes sense, in our opinion, to allow scale changes when combining measurements of a single physical type.) While one might think of the polyhedron as being aligned and oriented with an external reference frame during a Helmert transformation, it is typically more useful to consider the frame (axis system) as the entity undergoing the change in position and orientation. That is, we are really transforming the coordinates of

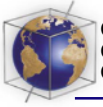


the stations composing the polyhedron from those associated with the arbitrary reference frame invoked by (or implicit in) the free network solution to those associated with a conventional reference frame such as the International Terrestrial Reference Frame (ITRF) or a fixed-plate frame. Inner geometry is invariant under translation and rotation of the reference frame, whereas station coordinates are not.

[8] Crustal motion geodesists are mainly concerned with estimating the velocities of their GPS stations in some well-defined reference frame. A series of free network solutions obtained over a sufficiently long time span (usually 2 years or more) implies how the internal geometry of the polyhedron changes over time. Just as the instantaneous geometry of the polyhedron can be conceived of in terms of its inner and outer geometry, so the deformation of the polyhedron, i.e., the motions of its stations, can be analyzed in terms of its inner or outer geometry [Blewitt *et al.*, 1993]. Ultimately, we will require the station velocities to be expressed in a conventional reference frame. There are two general approaches to doing this. The older (and probably still more widely used) approach is to transform each daily polyhedron into a conventional reference frame, such as ITRF, and then estimate the station velocities in that reference frame. In practice the reference frame is realized over an extended period of time by strongly constraining the positions and velocities of the IGS stations to their ITRF values. The alternative approach, which we prefer, is to estimate positions and velocities in inner coordinates, treating the reference frame merely as a computational convenience, and allowing it to rotate and translate freely (at constant rates) while focusing on the rate of change of the polyhedron's shape and size. We transform the resulting inner coordinate solution (positions and velocities) into a conventional reference frame only after velocity estimation has been completed. This is

achieved by finding a suitable 12 parameter transformation consisting of three rotations, three rotation rates, three translations, and three translation rates. This generalized Helmert transformation relates any two reference frames over an extended period of time, just as the six parameter Helmert transformation relates any two reference frames at a given moment or epoch. (Some workers, such as Boucher *et al.* [1998] and Davies and Blewitt [2000], employ 14 parameter generalized Helmert transformations instead, so as to allow scale and scale rate differences between reference frames.) The advantage of inner coordinate velocity estimation, like that of the free network solution, is that it eliminates the potentially harmful influence of prior information (in this case prior velocity information). We consider inner coordinate velocity estimation to be the logical extension of the free network approach to the analysis of a network over an extended period of time.

[9] We perform inner coordinate position and velocity estimation using our own software package called VSTACK. One six parameter Helmert transformation is applied to each daily polyhedron solution so as to align the daily polyhedra as closely as possible to a suite of constant velocity trajectories (unless an earthquake requires the introduction of additional coseismic steps at nearby stations). No position or velocity constraints are imposed during this iterative stacking process: the only constraint is that the individual (daily) polyhedra are not allowed to change their size or shape. Our algorithm is most easily understood by considering the simple case of a polyhedron time series in which no coseismic (or other) jumps occur. We can visualize the algorithm in the following way. First we estimate the velocity of each station by fitting a straight line to each of its spatial (cartesian) coordinates as a function of time. We then seek a set of Helmert transformations, one for each day, that align all



stations occupied on a given day as well as possible with these station trajectories (linear position versus time fits). This process is iterated: we reestimate the three velocity components for each station and then repeat the stacking or alignment process. At each iteration we track the individual and composite distances between the stations and the network position-velocity model and terminate iteration when a specific target is reached or when no further progress is being made toward convergence.

[10] After stacking and velocity estimation is completed, we realize a craton- or plate-fixed frame, i.e., one which is nominally attached to the stable (effectively rigid) core of a plate, by performing a generalized Helmert transformation which minimizes the horizontal and vertical velocities of a set of stations located within the stable part of the plate and optionally by minimizing simultaneously the vertical velocities of a second set of stations located in the stable cores of adjacent plates. That is, we estimate the 12 parameters of the transformation so as to minimize a composite measure of these residual velocities in the new frame. Plate stability can be assessed a posteriori by examining the residual velocities in this plate-fixed frame. (A similar approach can be used to transform our solution into ITRF: we choose the 12 parameters of the transformation so as to minimize the weighted deviations of all IGS station positions and velocities from those values assigned to them in the ITRF frame).

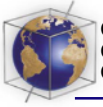
[11] A key feature of our approach to regional velocity analysis is that even though we use GAMIT/GLOBK to estimate a daily polyhedron that includes both our regional stations and the global tracking network of the IGS, we subsequently extract a regional subset of these stations for the purpose of velocity estimation. This subset consists of all stations in the South American plate, all stations in the Nazca plate, and only a few stations located in immediately

adjacent plates. We stack on a regional basis because, as we found previously in the South Pacific [e.g., *Bevis et al.*, 1995], and as *Wdowski et al.* [1997] found in California, global stacking admits significant amounts of spatially coherent noise into our regional time series [*Kendrick et al.*, 1999]. Systematic errors enter into a velocity analysis from all spatial scales, and there is some advantage to limiting the aperture of the network being analyzed to that of the specific region under study.

[12] The set of stations we use to realize a South American craton-fixed frame in this paper (Table 1) differs from that we used previously [*Kendrick et al.*, 1999; *Bevis et al.*, 1999] in that we now appreciate that the continuous station (PARC) in Punta Arenas (southernmost Chile) lies just within, rather than just outside, the active Patagonian Fold and Thrust Belt, and so it does not lie within the craton. Accordingly, we have dropped this station in favor of a relatively new CGPS station (LKTH) located at Lookout Hill in the Falkland Islands and a longer established rover GPS station (TNDL) located in Tandil, Argentina. The RMS residual velocity of this group of stations is just 1.1 mm/yr. If we exclude the rover station TNDL, then the RMS velocity of the eight remaining CGPS stations is 1.0 mm/yr.

3. A Combined Velocity Field

[13] The data set analyzed by *Norabuena et al.* [1998] was based on two GPS campaigns mounted in 1994 and 1996, and, as a result, the total observational time span at each of the SNAPP stations was just over 2 years. In contrast, the nearby CAP stations in northernmost Chile and Argentina analyzed by *Bevis et al.* [1999] had a minimum occupation time of ~ 3.6 years. As part of an effort to better tie the CAP and SNAPP networks, in late 1999 the CAP team reoccupied a station (CATA) it

**Table 1.** Continuous and Rover GPS Stations Used by the Pacific GPS Facility (PGF) to Realize a Craton-Fixed Reference Frame^a

Code	Location	Lat	Long	Nobs	Tspan	Vn	sigVn	Ve	sigVe	Typ
KOUR	Kourou	5.25	-52.81	2142	8.17	-0.4	0.2	0.8	0.4	I
FORT	Fortaleza	-3.88	-38.43	2378	7.64	0.3	0.1	-0.4	0.4	I
BRAZ	Brazilia	-15.95	-47.88	1050	5.95	0.1	0.3	1.0	0.5	I
UEPP	Pr. Prudente	-22.12	-51.41	1180	5.57	0.5	0.3	-1.2	0.5	B
PARA	Curitiba	-25.45	-49.23	1153	5.58	0.4	0.3	-0.6	0.4	B
LPGS	La Plata	-34.91	-57.93	1663	7.14	-0.8	0.2	-0.5	0.2	I
LHCL	Lihue Calel	-38.00	-65.60	1173	4.23	-1.0	0.2	-0.8	0.2	C
LKTH	Lookout Hill	-51.70	-57.85	529	2.35	1.0	0.5	-0.1	0.4	C
TNDL	Tandil	-37.32	-59.09	13	5.66	-0.1	1.6	1.7	1.5	R

^aFor each station we list the station code, location, latitude and longitude, the number of daily observations incorporated into the geodetic analysis, the total time spanned by these observations (in years), the north component of velocity (Vn) and its standard error (sigVn), the east component of velocity (Ve) and its standard error (sigVe), and the station type (I, IGS global tracking station; B, CGPS station of the Instituto Brasileiro de Geografia e Estatística; C, CGPS station associated with CAP; R, CAP rover station). RMS residual velocity (9 stations) = 1.1 mm/yr.

established in western Bolivia in early 1993 and simultaneously occupied the nearby SNAPP station PNAS. And in early 2000, a CAP survey crew that reoccupied stations YAVI and TRES in northern Argentina also occupied five SNAPP stations in southern Bolivia, two of which (PSUC and SJCH) are located in the craton. These data, and data from the northern CAP network, will be used by both groups to establish a small subset of stations, which are shared and, hopefully, will be occupied more frequently than other rover stations in the region. In this way the CAP and SNAPP networks will be strongly tied together.

[14] We processed the SNAPP and northern CAP networks jointly and estimated the velocities of all stations in the craton-fixed frame of reference described above. We present velocities only for those CAP stations north of $\sim 23^{\circ}\text{S}$, since the stations further south were displaced by the Antofagasta earthquake [Klotz *et al.*, 1996, 1999] and are not very useful for characterizing the interseismic velocity field. We estimated velocities using only the SNAPP data available to Norabuena *et al.* [1998] and using in addition the more recent data from the “tie” stations. The two

sets of velocity solutions differ only slightly, though the stations with additional recent occupations have smaller error ellipses when the recent data are included in the velocity analysis. A comparison of the new solutions for the SNAPP stations and those published previously by Norabuena *et al.* [1998], confirms that the original solution has a 7.5 mm/yr bias in the eastward component of velocity. The corresponding bias in the north component of velocity is only -0.3 mm/yr, which is negligible. These bias estimates, which represent median differences between the old and new solutions (old–new) for the set of common stations, are insensitive to the inclusion or exclusion of the post-1996 observations at the SNAPP sites.

[15] The integrated velocity field is shown in Figure 1 and listed in Table 2. Note that five of the six SNAPP stations located in the craton (PSUC, INGM, SJCH, REYE, and FITZ) have velocities that differ from zero at a level which is not statistically significant or only barely significant. This set of stations has an RMS residual velocity of 2.7 mm/yr. The sixth cratonic station RBLT has north and east components of velocity of 5.3 ± 1.9 and 0.9 ± 3.4 mm/

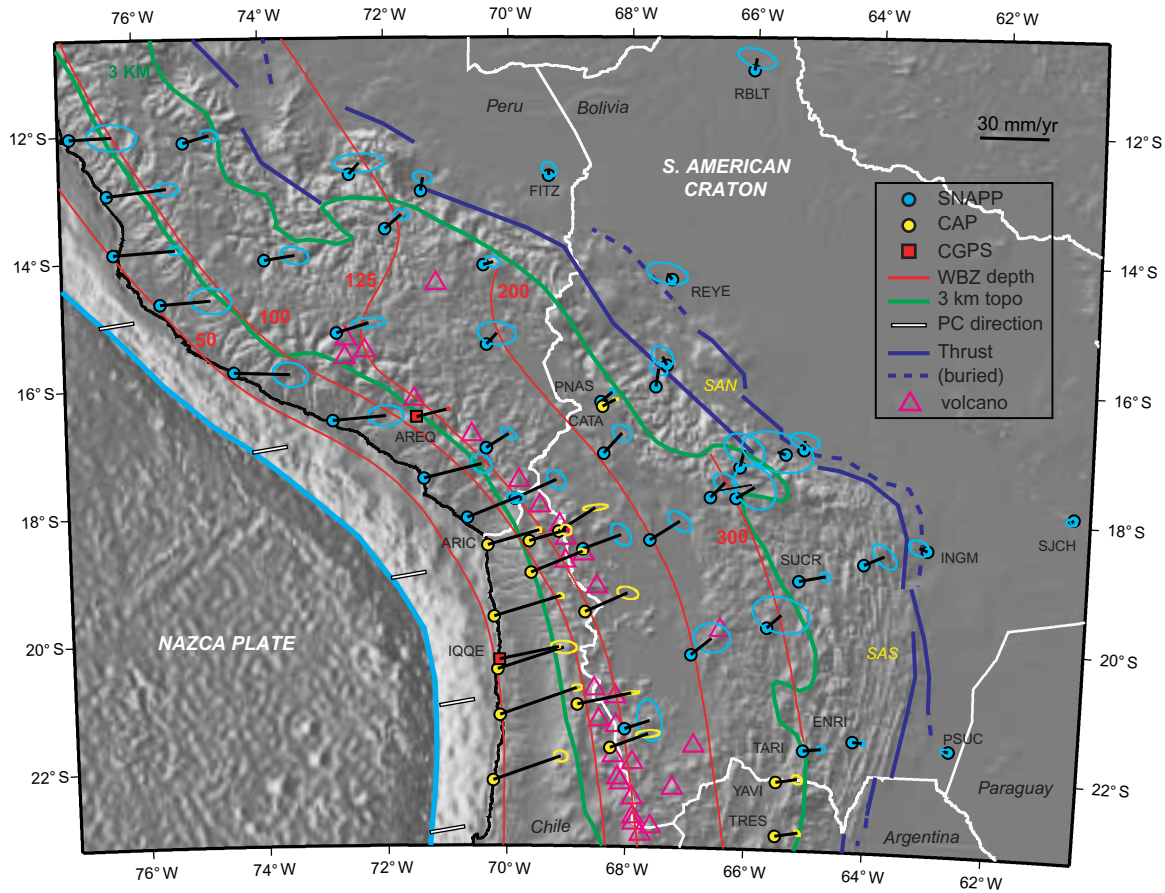
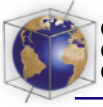


Figure 1. The integrated crustal velocity field for the central Andes, north of 23°S, relative to the stable core of the South American plate. Stations belonging to the SNAPP and CAP networks are colored blue and yellow respectively. The error ellipses are nominally 95% confidence ellipses. The light blue curve is the trench axis. The red curves are the *Cahill and Isacks* [1992] depth contours for the middle of the Wadati-Benioff zone. The green curve is a highly smoothed version of the 3 km elevation contour. The outermost thrusts of the back arc (foreland) region are shown in dark blue: solid lines indicate thrust faults which break the surface, whereas dashed lines indicate buried or blind thrusts, some of which are inferred rather than observed. The open triangles indicate the active volcanic arc. The white rectangles near the trench axis indicate the direction, but not the magnitude, of Nazca - South America plate convergence. These directions are predicted using an Euler vector derived from GPS measurements (as we will describe elsewhere). The components of this vector, expressed in geocentric coordinates, are $[-0.191006, -4.66105, 8.78279] \times 10^{-9}$ radians/yr. Abbreviations used in the figure: SAN, the northern Subandean zone; SAS, the southern Subandean zone.

yr, respectively, which gives it a statistically significant northward component of motion but no significant eastward component of motion. Note that none of these stations were used in the definition or realization of the craton-fixed

frame. Since these stations appear fixed, or very nearly fixed, even though this result was in no way built into the solution, we feel confident that the SNAPP stations are properly integrated into our regional reference frame.

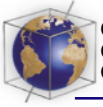
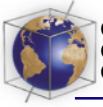


Table 2. The Integrated Velocity Solution for the CAP and SNAPP Networks of the Central Andes (See Figure 1)^a

Code	Lat	Long	Vn	SigVn	Ve	SigVe	neCor	Tspan	Net
ANCQ	-19.53	-68.72	8.3	1.1	18.3	1.9	-0.293	3.7	C
AREQ	-16.47	-71.49	3.3	0.1	13.2	0.1	-0.221	6.9	I
ARIC	-18.48	-70.33	6.4	0.4	22.1	0.4	-0.190	6.8	C
AYRO	-17.75	-69.88	8.1	1.7	17.7	1.7	-0.347	2.1	S
BAJO	-16.95	-70.35	6.0	1.0	9.6	1.5	-0.625	2.2	S
CANA	-13.99	-73.93	2.0	1.5	13.2	2.4	-0.224	2.2	S
CASM	-9.45	-78.31	-6.9	0.8	-6.3	2.0	-0.071	2.1	S
CATA	-16.30	-68.46	3.0	0.2	5.6	0.5	0.021	6.8	C
CHIM	-16.94	-65.17	4.1	1.4	0.2	2.6	-0.274	2.1	S
CHNG	-18.26	-69.17	10.2	0.6	15.7	2.2	0.458	3.7	C
CHTA	-20.17	-66.95	7.3	2.5	8.8	3.2	-0.035	2.1	S
CMOR	-18.05	-70.66	8.3	0.8	20.6	1.5	-0.123	2.1	S
CNOR	-17.23	-66.21	7.8	2.8	1.8	3.6	-0.333	2.1	S
COMA	-17.04	-68.44	8.7	1.5	7.8	1.6	-0.245	2.1	S
CORQ	-18.39	-67.66	8.2	1.8	12.7	2.1	-0.512	2.1	S
COTA	-15.14	-72.78	4.2	0.9	13.9	2.9	0.227	2.1	S
CSUR	-17.72	-66.27	4.9	3.9	8.0	3.8	-0.254	2.1	S
CUSO	-13.51	-71.98	6.1	0.9	7.1	1.3	-0.092	2.2	S
ENRI	-21.47	-64.23	-0.3	0.4	4.1	0.5	-0.173	6.4	S
FITZ	-12.67	-69.35	2.5	1.2	0.1	1.3	-0.233	2.2	S
GRIN	-18.42	-69.64	4.7	0.9	15.8	0.9	-0.202	3.1	C
HUAN	-12.13	-75.21	3.2	1.0	11.4	1.5	-0.233	2.2	S
INGM	-18.46	-63.12	1.4	1.4	-3.6	1.8	-0.319	2.1	S
IQQE	-20.27	-70.13	5.4	0.1	25.4	0.2	-0.275	4.6	C
JHAI	-16.52	-72.86	1.9	1.8	22.9	3.1	0.001	2.1	S
LAMP	-15.33	-70.35	4.7	2.0	4.4	3.4	-0.131	2.1	S
LEON	-15.99	-67.60	7.7	1.1	1.1	1.5	-0.335	2.1	S
MACU	-14.08	-70.40	1.2	1.1	4.3	1.3	-0.324	2.1	S
OLLA	-21.35	-68.04	3.7	3.6	10.7	2.2	-0.204	2.1	S
ORUR	-17.71	-66.69	6.5	1.6	6.2	2.0	-0.326	2.1	S
PBLN	-22.17	-70.23	10.3	1.0	28.9	1.2	-0.129	3.7	C
PNAS	-16.23	-68.49	4.1	0.5	4.8	0.4	-0.089	5.6	S
POCO	-17.43	-71.37	6.1	1.7	24.7	1.8	-0.311	2.1	S
POTO	-19.73	-65.71	5.6	3.2	6.1	5.0	-0.217	2.1	S
PPAT	-12.91	-71.41	5.7	1.1	1.0	1.6	-0.245	2.1	S
PPST	-20.98	-68.83	5.0	0.3	23.2	1.4	0.609	3.7	C
PRAC	-13.87	-76.36	1.6	0.8	26.7	1.2	-0.067	2.1	S
PSAG	-19.60	-70.22	8.8	0.5	28.5	0.6	-0.273	3.7	C
PSUC	-21.56	-62.63	0.3	0.5	-1.8	0.6	-0.328	6.4	S
PTCH	-21.15	-70.12	11.7	0.5	32.9	0.9	0.134	3.8	C
PUCA	-8.40	-74.67	0.5	1.1	-2.8	2.3	-0.024	2.1	S
QLLO	-12.65	-72.56	4.8	1.7	4.3	4.4	0.140	2.1	S
QUIL	-12.95	-76.44	2.8	1.2	25.7	2.1	-0.028	2.2	S
RBLT	-11.01	-66.07	5.3	1.9	0.9	3.4	-0.445	2.1	S
REYE	-14.30	-67.35	2.5	2.0	-2.2	3.6	-0.348	2.1	S
SACA	-18.54	-68.76	6.2	1.9	16.3	1.8	-0.406	2.1	S
SAPE	-15.65	-67.42	3.7	1.9	-2.0	2.0	-0.331	2.1	S
SCNA	-18.91	-69.62	9.1	0.3	22.0	0.6	-0.283	3.7	C
SCRI	-12.04	-77.02	0.6	2.3	18.3	4.4	-0.062	2.1	S
SJCH	-17.87	-60.77	-0.9	0.6	-1.0	0.9	-0.093	6.4	S
SLAS	-21.65	-68.28	6.2	0.7	16.3	2.0	0.282	3.7	C
SUCR	-18.99	-65.21	2.4	0.8	11.4	0.9	-0.243	6.4	S
TANA	-15.75	-74.45	-1.0	2.2	24.2	3.1	-0.155	2.1	S

**Table 2.** (continued)

Code	Lat	Long	Vn	SigVn	Ve	SigVe	neCor	Tspan	Net
TARI	-21.63	-65.05	0.9	0.6	7.8	0.8	-0.024	6.4	S
TRES	-22.98	-65.48	1.7	0.5	9.8	0.5	-0.626	7.1	C
TUNA	-17.02	-65.47	1.1	3.6	-3.6	6.3	-0.284	2.1	S
VAGR	-18.71	-64.15	4.0	2.2	8.8	2.2	-0.587	2.1	S
VRDS	-20.43	-70.16	9.4	1.1	28.4	2.3	-0.085	3.7	C
YAVI	-22.14	-65.49	1.5	0.8	9.2	0.9	-0.288	7.1	C
ZAMA	-14.66	-75.62	1.4	2.3	21.8	3.5	-0.117	2.1	S

^aThese velocities are expressed relative to the stable core of the South American plate. For each station we provide its 4-letter code, its latitude and longitude, the north component of velocity and its standard error (in mm/yr), the east component of velocity and its standard error, the correlation between the north and east components of velocity error (which specifies the orientation of the error ellipse), the total time span of observations in years, and the network to which the station belongs (S, SNAPP; C, CAP; I, IGS).

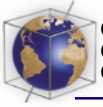
[16] The solutions for nearly collocated stations PNAS and CATA, in western Bolivia, are very similar. This is significant in that CATA has one of the best-constrained velocity solutions for any rover GPS station in the CAP network, since its total observational time span is 6.8 years (though YAVI and TRES in northern Argentina have even better solutions since they have been occupied three times over more than seven years). A visual inspection of the velocity field shows that the velocity discontinuity (near the boundary of the CAP and SNAPP networks) apparent in the plots of *Bevis et al.* [1999] is no longer evident. We conclude that our new, integrated velocity field is considerably more useful than one obtained by combining the previously published results of *Norabuena et al.* [1998] and *Bevis et al.* [1999]. We recommend use of the new solution as an interim interseismic velocity field for the central Andes.

4. Discussion

[17] On 23 June 2001, after this research was completed, an M_W 8.4 earthquake ruptured the plate boundary near 17.2°S , 73.0°W . All of the GPS data analyzed in this study was collected prior to the occurrence of this great earthquake, and so the velocity results presented here can

be used to address only the interseismic phase of the earthquake deformation cycle that preceded this seismic event. Because SNAPP performed additional occupations of their network just prior to 23 June 2001 (Tim Dixon, personal communication, 2001), it is likely that this interim velocity field will be superceded. No further occupation of the CAP stations in northernmost Chile took place prior to this great earthquake, so our solutions for the interseismic velocity field at those stations are unlikely to be modified in a significant way.

[18] The *Norabuena et al.* [1998] solution for the interseismic velocity field implied that ~ 10 – 15 mm/yr of Nazca, South America plate convergence across the central Andes takes place in the back arc region and that only about half of the convergence occurring at the main plate boundary was associated with elastic strain accumulation due to a locked plate boundary. In their model ~ 34 – 42% of the plate convergence was occurring aseismically, so the main plate boundary was only partially coupled or locked. These findings require some revision in light of the new velocity field. Since most of the stations in Peru and Bolivia have had their eastward component of velocity reduced by ~ 7.5 mm/yr relative to the solution of *Norabuena et al.* [1998], it follows that the fraction of plate convergence taking place in the back



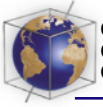
arc was probably smaller than previously suggested and that the degree of coupling or locking at the main plate boundary was probably somewhat larger than previously reported. These conclusions are borne out by modeling studies based on the newly integrated velocity field [Bevis *et al.*, 2001].

Acknowledgments

[19] We are very grateful to Tim Dixon and Seth Stein for inviting us to reprocess their SNAPP data along with our CAP data in order to address the reference frame problem identified by Bevis *et al.* [1999]. We thank Mauro Blanco and Pablo Euillades of CEDIAC at the Universidad Nacional de Cuyo, the Instituto Geográfico Militar de Chile, the Instituto Geográfico Militar de Argentina, Parques Nacionales de Argentina, and the Department of Agriculture in the Falklands Islands, for participating in our recent field measurements and/or operating continuous GPS stations. We thank Shimon Wdowinski and the Instituto Geográfico Militar de Bolivia for organizing the 1993 occupation of station CATA. We gratefully acknowledge the logistical assistance of UNAVCO during our 1993 field campaign. The Instituto Brasileiro de Geografia e Estatística kindly provided us with data from their CGPS stations PARA and UEPP. We thank Geoffery Blewitt, Tom Herring, and Simon Lamb for their useful comments and suggestions. Robert Reilinger provided us with a very detailed and thoughtful review, for which we thank him. This research was supported by the National Science Foundation through grants EAR-9116733, EAR-9512212 and EAR-9596061. This is SOEST contribution 5835 and CERI contribution 435.

References

- Bevis, M., *et al.*, Geodetic observations of very rapid convergence and back-arc extension at the Tonga island arc, *Nature*, **374**, 249–251, 1995.
- Bevis, M., E. Kendrick, R. Smalley, T. Herring, J. Godoy, and F. Galban, Crustal motion north and south of the Arica deflection: Comparing recent geodetic results from the Central Andes, *Geochem. Geophys. Geosyst.*, **1**, Paper 1999GC000011, 1999. (Available at <http://g-cubed.org>)
- Bevis, M., E. Kendrick, R. Smalley, B. Brooks, R. Allmendinger, and B. Isacks, On the strength of interplate coupling and the rate of backarc convergence in the Central Andes: An analysis of the interseismic velocity field, *Geochem. Geophys. Geosyst.*, **2**, 2001. (Available at <http://g-cubed.org>)
- Blewitt, G., GPS data processing methodology: From theory to applications, in *GPS for Geodesy*, edited by P. Teunissen and A. Kleusberg, pp. 231–270, Springer-Verlag, New York, 1998.
- Blewitt, G., M. Heflin, Y. Vigue, J. Zumberge, D. Jefferson, and F. Webb, The Earth viewed as a deforming polyhedron: Method and results, in *Proceedings of the 1993 IGS Workshop*, edited by G. Beutler and E. Brockmann, pp. 165–174, Univ. of Berne, Bern, Switzerland, 1993.
- Bock, Y., Medium distance GPS measurements, in *GPS for Geodesy*, edited by P. Teunissen and A. Kleusberg, pp. 484–536, Springer-Verlag, New York, 1998.
- Boucher, C., Z. Altamimi, and P. Sillard, Results and analysis of the ITRF96, *Tech. Note 24*, 166 pp., Int. Earth Rot. Serv., Paris, 1998.
- Cahill, T., and B. L. Isacks, Seismicity and shape of the subducted Nazca plate, *J. Geophys. Res.*, **97**, 17,503–17,529, 1992.
- Davies, P., and G. Blewitt, Methodology for global geodetic time series estimation: A new tool for geodynamics, *J. Geophys. Res.*, **105**, 11,083–11,100, 2000.
- Feigl, K., *et al.*, Space geodetic measurement of crustal deformation in central and southern California, 1984–1992, *J. Geophys. Res.*, **89**, 21,677–21,712, 1993.
- Gephart, J., Topography and subduction geometry in the central Andes: Clues to the mechanics of a noncollisional orogen, *J. Geophys. Res.*, **99**, 12,279–12,288, 1994.
- Heflin, M., *et al.*, Global geodesy using GPS without fiducial sites, *Geophys. Res. Lett.*, **19**, 131–134, 1992.
- Herring, T., Documentation for GLOBK: Global Kalman Filter VLBI and GPS analysis program, Version 10.0, MIT, 2000.
- Isacks, B., Uplift of the central Andean plateau and bending of the Bolivian orocline, *J. Geophys. Res.*, **93**, 3211–3231, 1988.
- Jordan, T., B. Isacks, R. Allmendinger, J. Brewer, V. Ramos, and C. Ando, Andean tectonics related to geometry of the subducted Nazca plate, *Geol. Soc. Am. Bull.*, **94**, 341–361, 1983.
- Kendrick, E., M. Bevis, R. Smalley, O. Cifuentes, and F. Galban, Current rates of convergence across the Central Andes: Estimates from continuous GPS observations, *Geophys. Res. Lett.*, **26**, 541–544, 1999.
- King, R., and Y. Bock, Documentation for the GAMIT GPS Analysis Software, Release 10.0, MIT and Scripps Inst. of Oceanogr., Cambridge, Mass., 2000.
- Kley, J., Geologic and geometric constraints on a kinematic model of the Bolivian orocline, *J. South Am. Earth Sci.*, **12**, 221–235, 1999.
- Klotz, J., J. Reinking, and D. Angermann, Die vermessung der deformation der erdoberflaeche, *Geowissenschaften*, **14**, 389–394, 1996.



- Klotz, J., et al., GPS-derived deformation of the Central Andes including the 1995 Antofagasta $M_w = 8.0$ Earthquake, *Pure Appl. Geophys.*, *154*, 709–730, 1999.
- Lamb, S., Active deformation in the Bolivian Andes, South America, *J. Geophys. Res.*, *105*, 25,627–25,653, 2000.
- McCaffrey, R., Global variability in subduction thrust zone — forearc systems, *Pure Appl. Geophys.*, *142*, 173–224, 1994.
- Norabuena, E., L. Leffler-Griffin, A. Mao, T. Dixon, S. Stein, I. Sacks, L. Ocala, and M. Ellis, Space geodetic observation of Nazca - South America convergence across the Central Andes, *Science*, *279*, 358–362, 1998.
- Oral, M. B., Global Positioning System (GPS) measurements in Turkey (1988–1992): Kinematics of the Africa-Arabia-Eurasia plate collision zone, Ph.D. thesis, Mass. Inst. of Technol., Cambridge, 1994.
- Wdowinski, S., Y. Bock, J. Zhang, P. Fang, and J. Genrich, Southern California Permanent GPS Geodetic Array: Spatial filtering of daily positions for estimating coseismic and postseismic displacements induced by the 1992 Landers earthquake, *J. Geophys. Res.*, *102*, 18,057–18,070, 1997.
- Zhang, J., Continuous GPS measurements of crustal deformation in southern California, Ph.D. dissertation, Univ. of Calif., San Diego, 1996.